ELSEVIER

Journal of Nuclear Materials 275 (1999) 164–185

journal of nuclear materials

www.elsevier.nl/locate/jnucmat

A theoretical study of volatile fission products release from oxide fuels

M.C. Paraschiv [a,*], A. Paraschiv [a], V.V. Grecu [b]

[a] *Institute for Nuclear Research, P.O. Box 78, 0300, Pitesti, Romania*
[b] *University of Bucharest, Faculty of Physics, P.O. Box MG-11, Bucharest, Romania*

Received 25 June 1997; accepted 7 April 1999

Abstract

Treating the average volume grains as thermodynamically closed subsystems, a method to evaluate the volatile fission products migration at the grain boundary and their release in the void volume of the fuel elements is proposed. The method considers the phenomena of the intergranular bubble growth and interlinkage, grain growth and grain boundary resolution. Analytical solutions of the diffusion problem associated with the volatile fission products behaviour taking into account their direct yield from fission and from precursors simultaneously with the diffusion and decay, irradiation induced resolution and fuel grain growth, during a time-step varying irradiation history have also been derived. The results are very accurate and point out the strong effect of the boundary condition changes on the volatile fission products behaviour when the simultaneous effects of the intergranular bubble coalescence, the precursors, the irradiation induced resolution and grain growth are considered. Comparative analyses versus other similar models of the diffusion of only stable gas species of fission products are also presented.

1. Introduction

It is known that the microstructure of the fuel is intimately related to the behaviour of the fission gases, but how easy it is for fission gases to escape from the fuel once they have reached the grain boundary were a matter of much dispute [1]. Many attempts to improve the physical meaning of this complex process were made and extensive theoretical works were done [1–9]. Speight [2] showed that the intragranular bubbles which arise during the fuel irradiation are short time saturated with gas atoms and a stationary state is reached between the fission gas atoms which are trapped inside bubbles and the atoms that redissolve into the matrix because of the interaction between the intragranular bubbles and the fission fragments.

Special attention has been focused on the manner in which the Speight's treatment of the fission products resolution at the grain boundary can be quantified versus other processes simultaneously involved in their behaviour [3–10,12,18]. Thus, Turnbull and Friskney [4] changed the perfect sink boundary condition from the Booth sphere model [19], by an imperfect one and defined the grain boundary solute atom interaction energy of the volatile fission products to consider their chemical interaction with the fuel matrix. Forsberg and Massih [9] found the corresponding generalisation of the diffusion equation with a time dependent concentration on the grain boundary in the form of an integro-differential equation and gave rigorously analytical approximations for short times and long times, associated to the diffusion problem simultaneously with irradiation induced resolution.

The effect of grain growth on the fission gas diffusion at the grain boundary in oxide fuels has been firstly pointed out by Hargreaves and Collins [20], that consider a supplementary accumulation of fission gases at the grain boundary,

* Corresponding author.

0022-3115/99/$ - see front matter
PII: S0022-3115(99)00113-0

proportionally with the rate of grain growth. In a similar manner Notley and Hastings [25], developed a microstructure model of fission gas release that, for the first time, includes the material properties specific for a fuel manufacturer (Canadian fuel).

It is however difficult to point out the weights of the processes involved in fission products behaviour during a real irradiation history. A complete mathematical description in both steady state and transient fuel operating conditions would be necessary.

To this aim, in Refs. [11,12,15] a method of calculating diffusion of the stable fission gas species simultaneously with the grain growth in oxide fuels has been outlined. The method consists mainly of a new mass balance of the diffusing species using a time dependent coordinate system. Its main result was that for a better prediction of the fission gas behaviour, specific grain growth laws must be considered for every fuel manufacturer [11].

The method has been also extended to consider the irradiation induced resolution of the stable species of Xe and Kr at the fuel grain boundaries [12]. Based on Forsberg and Massih's mathematical formulation of the diffusion problem associated to the fission gas diffusion, the properties of the Heaviside function and the method of calculating the fission gas diffusion simultaneously with the grain growth, Paraschiv and Paraschiv [12] introduced the fission gas resolution at the grain boundary using a constant correction parameter to define the mass balance of stable fission gas species in a thermodynamically closed subsystem associated to the average volume grain. They found analytical solutions of the diffusion of stable fission gas species simultaneously considering the grain growth both in steady state and in transient irradiation conditions of the oxide fuel, in the form of the analytical approximations for short times and long times previously calculated by Forsberg and Massih [9]. Based on these, they proved the effect of grain growth on the incubation times of the intergranular bubble coalescence.

Special studies were dedicated to the manner in which a grain volume distribution function could influence the fission gas release [13,14]. For a continuous distribution of the fuel grains, the irradiation induced resolution involves the same volatile fission products surface concentration at the boundary of any fuel grain, if the thermodynamic forces on grain boundary are the same anywhere at the fuel grain boundaries. This assumption becomes very useful when the real grain volume distribution function is accounted for [14]. The method described above has been also applied to describe the volatile fission products behaviour inside the oxide fuel, but only for the simple case of the Booth sphere model (zero boundary condition for gas diffusion at the grain boundary) [15].

The purpose of this paper is to present an extension of the method to the volatile fission products behaviour during a step-wise irradiation history of the oxide fuel. The following processes are considered:

- Fission products yielding directly as fission fragments or from precursors.
- Migration of fission products at the grain boundary by both diffusion and sweeping.
- Intergranular bubbles growing and interlinkage as a result of the migration at the grain boundary of the stable species of Xe and Kr (the major components of the fission gas).
- Irradiation induced resolution at the grain boundary corresponding to every decay chain as a time-step dependent function.

All the above mentioned processes occur in a polycrystal that can alternatively be characterised by a grain volume distribution function and whose grain boundaries move in time during a time-varying irradiation history.

2. Statement of the problem

Taking into account that the stable species of Xe and Kr give the main contribution of the fission gas release in the void volume of the fuel element [1], the behaviour of an arbitrary volatile fission species, k, can be treated using, with only few changes, the method previously proposed in Ref. [12]. Thus, we will use below the assumption that the average volume grain can be treated at any time-step, grain growth-controlled or temperature-controlled, as a thermodynamically homogeneous closed subsystem (there is no mass transfer with the surrounding of any component). Then, from the conservation condition of the total number of the atoms of an arbitrary species k, the number of atoms which remain at any time at the grain boundary is

$$N_{\mathrm{l}}^{k}(t) = Q_{\mathrm{T}}^{\prime k} - N_{\mathrm{r}}^{k} - N^{k}, \tag{1}$$

where $Q_{\mathrm{T}}^{\prime k}$ is the total amount of gas atoms of species k, generated in the fuel grain, N^k the amount of species k from the fuel grain and N_{r}^{k} is the amount of species k vented out from the grain boundary to the void volume of the fuel element.

Assuming an homogeneous yielding of species k inside the fuel grains, there will result that the total amount of species k generated inside the topological suitable sphere associated with the average volume grain up to the time t, can be written as

$$Q_{\mathrm{T}}^{k} = \frac{4\pi a_L^3}{3} n^k(t_L). \tag{2}$$

Similiar as in Ref. [15], build-up and decay of fission products of species k, inside the unit volume of the fuel $n^k(t)$, is described by a system of coupled differential equations whose solutions for an arbitrary linearized decay chain during a stepwise irradiation history is

$$n^k(t_L) = \sum_{l=1}^{k} P_l^k \left[n^l(t_{L-1}) \sum_{j=1}^{k} \frac{\mathrm{e}^{-\lambda_j\ \Delta t_L}}{\prod_{\substack{i=1 \\ i\neq j}}^{k} (\lambda_i - \lambda_j)} + \gamma_l F(t_L) \sum_{j=1}^{k} \frac{1 - \mathrm{e}^{-\lambda_j\ \Delta t_L}}{\lambda_j \prod_{\substack{i=1 \\ i\neq j}}^{k} (\lambda_i - \lambda_j)} \right]; \quad P_l^k = \prod_{i=1}^{k} \eta_{i-1}^i \lambda_{i-1}, \tag{3}$$

where η_{i-1}^i is the build-up of nuclide i, by unit decay and/or by unit neutron reaction of nuclide $i-1$,

$$\eta_{i-1}^i = f_{i-1}^i \frac{\lambda_{i-1}^*}{\lambda_{i-1}} + g_{i-1}^i \frac{\sigma_{i-1}\varphi(t)}{\lambda_{i-1}}; \quad \lambda_{i-1} = \lambda_{i-1}^* + \sigma_{i-1}\varphi(t). \tag{3a}$$

f_{i-1}^i is the build-up of nuclide i by unit decay nuclide $i-1$, g_{i-1}^i build-up of nuclide i, by unit neutron reaction, λ_{i-1}^* the decay constant of nuclide $i-1$, γ^l the fission yield of nuclide l, σ_{i-1} the average microscopic neutron reaction cross section of nuclide $i-1$, $\varphi(t)$ the neutron flux and $F(t)$ the fission rate (assumed constant on the time-step $\Delta t_L = t_L - t_{L-1}$).

Taking into account that the total number of the fuel grains will change in time as a result of grain growth, a new configuration of closed subsystems must be defined at any time-step. Thus, if some boundaries between the fuel grains were at a previous time inside the topological suitable volume associated with the new average grain volume, they will be moved out during irradiation.

Simultaneously with the fission products diffusion, a population of intergranular gas bubbles nucleate and grow until they interlink and the volatile fission products are vented out in the void volume of the fuel element. Many authors [9,16] have shown that a saturation of the grain boundaries with gas atoms of stable Xe and Kr species can be defined when the intergranular bubbles interlink and the fission gas is vented out.

Because of the external forces, the intergranular bubbles disappear after the fission gas release from the grain boundary. As long as new fission products arrive at the grain boundaries, a new bubble population will nucleate and grow.

The problems mentioned above can be considered by an adequate balance of the amount of the diffusing species k, inside the closed subsystem described above. That means that if N_j^{sk} atoms of species k, have been released in the void volume of the fuel element from the average volume grain corresponding to a previous time-step t_j, using the classical approximation of a fixed number of fuel grains of the same volume as the average volume grain N_{gr}, the contribution to the fission gas released from the unit volume will be

$$n_{\mathrm{r},j}^{\mathrm{k}} = \mathrm{N}_j^{\mathrm{s},k} N_{\mathrm{gr}}^j = \frac{3}{4\pi a_j^3} N_j^{\mathrm{sk}}, \tag{4}$$

where a_j is the radius of the average volume grain at the time-step t_j.

With only few changes, $n_{\mathrm{r,j}}^k$ can also be calculated using the grain volume distribution function that is specific for every fuel manufacturer [14]. Thus let $g_j(V)$ be specific grain volume distribution function at the time-step t_j, corresponding to a spherical form of the fuel grains and normalised to the unit volume. Then the contribution from the unit fuel volume to the fission gas release in the void volume of the fuel element is given by,

$$n_{\mathrm{r},j}^k = \frac{N_j^{\mathrm{s,k}}}{\bar{a}_j^2} \frac{1}{2} \int_0^\infty a^2 g(a^3)\ \mathrm{d}a^3. \tag{4a}$$

The factor 1/2 in Eq. (4a) has been introduced to take into account that the separation surface is shared in every point by two neighbouring grains.

Besides the amount of species k, released in the void volume of the fuel element it also yields from its precursors and decays during the fuel irradiation, so that according to Eq. (3) at the current time t_L we have

$$n_{\mathrm{r}}^k(t_L) = \sum_{l=1}^{k} P_l^k n_{\mathrm{r}}^l(t_{L-1}) \sum_{j=1}^{k} \frac{\mathrm{e}^{-\lambda_j\ \Delta t_L}}{\prod_{\substack{i=1 \\ i\neq j}}^{k} (\lambda_i - \lambda_j)}, \tag{5}$$

where $n_r^l(t_{L-1})$ is the amount of species l, that has been vented out from the unit fuel volume up to the end of the times step t_{L-1}.

For an arbitrary decay chain, the diffusion equation for the fission product of index number, k, in the system of the boundary velocity v^a [15] is

$$\frac{\mathrm{d}C^k}{\mathrm{d}t} = \nabla(D_k^a \nabla C^k) - C^k \nabla v^{\mathrm{a}} - \lambda_k C^k + \gamma_k F + \eta_{k-1}^k \lambda_{k-1} C^{k-1}, \tag{6}$$

where D_k^{a} is the diffusion coefficient in the system of the boundary velocity, λ_k the decay constant, γ_k the fission yield of the species k and η_{k-1}^k build-up of the nuclide k as a result of the decay of the nuclide $k-1$, according to Eq. (3a).

Based on the Speight's definition of the gas concentration at the grain boundary [2], we defined the concentration of species k at the boundary of the average volume grain [12] as,

$$C^k[a(t),t] = \varphi^k(t) = \mathrm{b}\frac{1}{V(t)}[Q_{\mathrm{T}}^k - N_{\mathrm{r}}^k - N^k(t)], \tag{7}$$

where $a(t)$ is the radius of the topological suitable sphere associated with the average volume grain $V(t)$. It has been previously calculated by Speight [2], that a saturation of the intragranular gas bubbles arises shortly after the beginning of the fuel irradiation and an effective diffusion coefficient can be defined for an accurate description of the gas diffusion at the grain boundary.

The correction parameter b introduced to simplify the form of Eq. (6) depends on the resolution parameter b', the surface–volume ratio ($S/V = 3/a(t)$ for a spherical geometry of the fuel grains) and the effective diffusion coefficient D^k. For a step-wise irradiation history all these are time-step-dependent. The effective diffusion coefficient depends on both the diffusing species k, and the intragranular bubbles resolution. On the other hand, because the volatile fission products yield and decay simultaneously with their diffusion in the fuel matrix, the contribution of every precursor from the decay chain to the isotope of interest is affected by its own diffusion properties. This implies a complicated form of the solution of diffusion and it becomes more useful to evaluate the effective diffusion coefficient D^k, from the experimental results for every decay chain of interest. For simplicity we will use in the following the notation $D^k = D$.

As it is mentioned by Olander [1], care must be taken in applying the resolution parameter because the form of the term representing resolution can depend on whether the bubbles can be completely destroyed by a single encounter with a fission fragment (Turnbull's model [1]) or gradually consumed by loss of individual gas atoms (Nelson's model [1]). Olander proved that for small bubbles the two models give the same value of the resolution parameter.

In both of them the resolution parameter b' is linearly dependent on fission rate and for larger intergranular bubbles a resolution efficiency has been defined by Nelson. Based on Olander calculations of the microscopic resolution parameter we can define

$$b' = 1.7 \times 10^{-17} \eta F \ (\mathrm{s}^{-1}); \quad \eta = 1 - \left\{1 - 15\left[\frac{1}{r_{\mathrm{b}}} + \frac{1}{B}\left(\frac{k_{\mathrm{B}}T}{2\gamma}\right)\right]\right\}^3; \quad B = 85 \ \mathring{A}^3 \tag{8}$$

where F is the fission rate and $r_{\mathrm{b}} > 5$ Å, the bubble radius. At the time-step t_L the correction parameter b can be written [12] as

$$b_L = \frac{\lambda b'_L a_L}{3D_L}, \tag{8'}$$

where λ is the resolution layer depth from the grain boundary (m) [2].

In order to simplify the solution method, the function $C(x,t)$ in Eq. (6) will be changed to

$$C'_k(x,t) = C^k(x,t) - C^k[a(t),t] = C^k(x,t) - \varphi^k(t). \tag{9}$$

The initial condition for a step-wise varying irradiation history can be written as

$$C'_k(x,0) = C'_k(x,0) - C^k[a(0),0] = C^k(x,t_{L-1}) - \varphi^k(t_{L-1}). \tag{9'}$$

Thus, Eq. (6) becomes

$$\frac{\mathrm{d}C'^k}{\mathrm{d}t} = \nabla_x(D^{\mathrm{a}}\nabla_x C^k) - C'^k \nabla_x v^{\mathrm{a}} - \varphi^k \nabla_x v^{\mathrm{a}} - \frac{\mathrm{d}\varphi^k}{\mathrm{d}t} - \lambda_k C'^k - \lambda_k \varphi^k + \gamma_k F + \eta_{k-1}^k \lambda_{k-1} C'^{k-1} + \eta_{k-1}^k \lambda_{k-1} \varphi^{k-1}, \tag{10}$$

where $\nabla_x = (\partial/(\partial x))$ is the divergence operator versus the coordinate system of the boundary velocity v^a.

Using the as-described transformation method to a fixed system [15], the 'diffusion equation' associated with the radioactive fission products diffusion simultaneously with the grain growth can be written as

$$\frac{\partial u^k}{\partial \tau} = \Delta_{x_0} u^k - \lambda'_k u^k + \frac{\gamma_k F'}{D'} + \eta_{k-1}^k \lambda'_{k-1} u^{k-1} - \frac{\mathrm{d}}{\mathrm{d}\tau}[\varphi^k J] - \lambda'_k[\varphi^k J] + \eta_{k-1}^k \lambda'_{k-1}[\varphi^{k-1} J], \tag{11}$$

where $\Delta_{x_0} = ((\partial^2)/(\partial x_0^2))$ = the Laplace operator,

$$\tau = \int_{t_L-1}^{t_L} \frac{D\mathrm{d}t}{a^2} \cong \frac{D_L \Delta t_L}{a_L^2}; \quad \lambda'_k = \frac{\lambda_k}{D'_L}$$

and

$$u^k(x_0,t) = C'^k(x,t)J(t),\ D'(t) = D(t)a^{-2}(t),\ \gamma_k F'(t) = \gamma_k F(t)J(t),\ J(t) = a^3(t). \tag{12}$$

$J(t)$ is the Jacobian of the transformation from the time dependent coordinate system to a fixed one [15]. From Eqs. (9) and (12), the total amount of species k, accumulated inside the fuel grain at any time is

$$N^k(t) = \int_{V(t)} C^k(x,t)\ \mathrm{d}V = \int_{V(t)} C'^k(x,t)\ \mathrm{d}V + \varphi^k(t)\ V(t) = \int_{V_0} u^k(x_0,t)\mathrm{d}V_0 + \varphi^k(t)\ V(t). \tag{13}$$

The solution of Eq. (11) can be written as a complete set of eigenfunctions,

$$u_k(x_0,\tau) = \sum_{n\geqslant 1} \Psi_n(x_0)K_n^k(\tau). \tag{14}$$

Taking into account that the eigenfunction and the eigenvalues of the Laplace operator satisfy equation,

$$\Delta_{x_0}\Psi_n(x_0) = -\lambda_n\Psi_n(x_0)$$

and based on the orthogonality properties of the eigensfunctions, Eq. (11) becomes

$$\frac{\mathrm{d}K_n^k}{\mathrm{d}\tau} = -(\lambda_n + \lambda'_k)K_n^k + \eta_{k-1}^k\lambda'_{k-1}K_n^{k-1} + u_n\left[\frac{\gamma_k F'}{D'} - \frac{\mathrm{d}}{\mathrm{d}\tau}(\varphi^k J) - \lambda'_k(\varphi^k J) + \eta_{k-1}^k\lambda'_{k-1}(\varphi^{k-1}J)\right], \tag{15}$$

where $u_n = \int_{V_0} \Psi_n(x_0)\ \mathrm{d}V_0$.

From Eqs. (7), (13) and (14) it follows

$$\varphi^k(t)J(t) = \frac{3}{4\pi}b[Q_T'^k - N_{\mathrm{r}}^k - N^k] = \frac{3}{4\pi}\frac{b}{1+b}\left[Q_{\mathrm{T}}^k(t) - \sum_{n\geqslant 1} u_n K_n^k(t)\right]; \quad Q_{\mathrm{T}}^k = Q_{\mathrm{T}}'^k - N_{\mathrm{r}}^k. \tag{16}$$

By Laplace transforming of Eq. (15) at an arbitrary time-step τ_L for constant size grain and constant fuel temperature and after a first arrangement of terms one obtains

$$\begin{aligned}\tilde{K}_n^k(p) - \frac{\frac{3}{4\pi}\frac{b_L}{1+b_L}(p+\lambda'_k)u_n}{p+\lambda'_k+\lambda_n}\sum_{m\geqslant 1} u_m\tilde{K}_m^k(p) = {} & \frac{K_n^k(\tau_0)}{p+\lambda'_k+\lambda_n} - \frac{\frac{3}{4\pi}\frac{b_{L-1}}{1+b_{L-1}}u_n}{p+\lambda'_k+\lambda_n}\sum_{m\geqslant 1} u_m K_m^k(\tau_0) \\ & + \frac{u_n\tilde{B}^k(p)}{p+\lambda'_k+\lambda_n} + \eta_{k-1}^k\lambda'_{k-1}\left[\frac{\tilde{K}_n^{k-1}(p)}{p+\lambda'_k+\lambda_n} - \frac{\frac{3}{4\pi}\frac{b_L}{1+b_L}u_n}{p+\lambda'_k+\lambda_n}\sum_{m\geqslant 1} u_m\tilde{K}_m^{k-1}(p)\right],\end{aligned} \tag{17}$$

where

$$\tilde{B}^k(p) = \frac{\gamma_k F'}{D'}\frac{1}{p} - \frac{3}{4\pi}\frac{b_L}{1+b_L}[(p+\lambda'_k)\tilde{Q}_{\mathrm{T}}^k(p) - \eta_{k-1}^k\lambda'_{k-1}\tilde{Q}_{\mathrm{T}}^{k-1}(p)] + \frac{3}{4\pi}\frac{b_{L-1}}{1+b_{L-1}}Q_{\mathrm{T}}^k(\tau_0). \tag{18}$$

Let us multiply Eq. (17) with eigenvalue u_n and note, $X_n^k(\tau) = u_n K_n^k(\tau)$. Then in Laplace space one obtains

$$\begin{aligned}\tilde{X}_n^k(p) - \frac{\frac{3}{4\pi}\frac{b_L}{1+b_L}(p+\lambda'_k)u_n^2}{p+\lambda'_k+\lambda_n}\sum_{m\geqslant 1}\tilde{X}_m^k(p) = {} & \frac{X_n^k(\tau_0)}{p+\lambda'_k+\lambda_n} - \frac{\frac{3u_n^2}{4\pi}\frac{b_{L-1}}{1+b_{L-1}}}{p+\lambda'_k+\lambda_n}\sum_{m\geqslant 1} X_m^k(\tau_0) \\ & + \frac{u_n^2\tilde{B}^k(p)}{p+\lambda'_k+\lambda_n} + \eta_{k-1}^k\lambda'_{k-1}\left[\frac{\tilde{X}_n^{k-1}(p)}{p+\lambda'_k+\lambda_n} - \frac{\frac{3u_n^2}{4\pi}\frac{b_L}{1+b_L}}{p+\lambda'_k+\lambda_n}\sum_{m\geqslant 1}\tilde{X}_m^{k-1}(p)\right].\end{aligned} \tag{19}$$

Let us also note

$$\tilde{X}(p+\lambda'_k) = \left[1 - \frac{3}{4\pi}\frac{b_L}{1+b_L}(p+\lambda'_k)\sum_{n\geqslant 1}\frac{u_n^2}{(p+\lambda'_k+\lambda_n)}\right]. \tag{20}$$

Because in Eq. (17) the index n has been arbitrarily chosen, a system of an infinite number of algebraic equations must be written, whose solutions have the form (see Appendix A)

$$\tilde{X}_n^k = \tilde{R}_n^k + \frac{3}{4\pi}\frac{b_L}{1+b_L}\frac{(p+\lambda_k')u_n^2}{[p+\lambda_k'+\lambda_n]\tilde{X}(p+\lambda_k')}\sum_{m\geqslant 1}\tilde{R}_m^k, \tag{21}$$

where

$$\tilde{R}_n^k(p) = \frac{X_n^k(\tau_0)}{(p+\lambda_k'+\lambda_n)} - \frac{\frac{3u_n^2}{4\pi}\frac{b_{L-1}}{1+b_{L-1}}}{(p+\lambda_k'+\lambda_n)}\sum_{m\geqslant 1}X_m^k(\tau_0) + \frac{u_n^2\tilde{B}^k(p)}{(p+\lambda_k'+\lambda_n)} + \eta_{k-1}^k\lambda_{k-1}'\left[\frac{\tilde{X}_n^{k-1}(p)}{(p+\lambda_k'+\lambda_n)} - \frac{\frac{3u_n^2}{4\pi}\frac{b}{1+b}}{(p+\lambda_k'+\lambda_n)}\sum_{m\geqslant 1}\tilde{X}_m^{k-1}(p)\right]. \tag{22}$$

Taking into account that in a spherical geometry $\lambda_n = (n\pi)^2$ and $u_n^2 = 8\pi/\lambda_n$, then Eq. (21) can be reduced to the form

$$\tilde{X}_n^k(p) = \frac{X_n^k(\tau_0)}{p+\lambda_k'+\lambda_n} - \frac{\frac{6b_L}{1+b_L}\sum_{m\geqslant 1}\frac{\lambda_m X_m^k(\tau_0)}{(p+\lambda_k'+\lambda_m)}}{\lambda_n(p+\lambda_k'+\lambda_n)\tilde{X}(p+\lambda_k')} + \frac{\left(\frac{6b_L}{1+b_L}-\frac{6b_{L-1}}{1+b_{L-1}}\right)\sum_{m\geqslant 1}X_m^k(\tau_0)}{\lambda_n(p+\lambda_k'+\lambda_n)\tilde{X}(p+\lambda_k')} + \frac{8\pi\tilde{B}^k(p)}{\lambda_n(p+\lambda_k'+\lambda_n)\tilde{X}(p+\lambda_k')} + \eta_{k-1}^k\lambda_{k-1}'\left[\frac{\tilde{X}_n^{k-1}(p)}{p+\lambda_k'+\lambda_n} - \frac{\frac{6b_L}{1+b_L}\sum_{m\geqslant 1}\frac{\lambda_m\tilde{X}_m^{k-1}(p)}{(p+\lambda_k'+\lambda_m)}}{\lambda_n(p+\lambda_k'+\lambda_n)\tilde{X}(p+\lambda_k')}\right]. \tag{23}$$

Eq. (23) for the first isotope of the decay chain becomes

$$\tilde{X}_n^1(p) = \frac{X_n^l(\tau_0)}{p+\lambda_1'+\lambda_n} - \frac{\frac{6b_L}{1+b_L}\sum_{m\geqslant 1}\frac{\lambda_m\tilde{X}_m^1(\tau_0)}{(p+\lambda_1'+\lambda_m)}}{\lambda_n(p+\lambda_1'+\lambda_n)\tilde{X}(p+\lambda_1')} + \frac{\left(\frac{6b_L}{1+b_L}-\frac{6b_{L-1}}{1+b_{L-1}}\right)\sum_{m\geqslant 1}X_m^1(\tau_0)}{\lambda_n(p+\lambda_1'+\lambda_n)\tilde{X}(p+\lambda_1')} + \frac{8\pi\tilde{B}^1(p)}{\lambda_n(p+\lambda_1'+\lambda_n)\tilde{X}(p+\lambda_1')}. \tag{24}$$

Using the substitution technique, from Eqs. (23) and (24) the solution of an arbitrary n, eigenfunction of the second isotope from the decay chain has the following form:

$$\tilde{X}_n^2(p) = \sum_{l=1}^{2}\sum_{j=1}^{2}\frac{P_l^2}{\prod_{\substack{i=l\\ i\neq j}}^{2}(\lambda_i'-\lambda_j')}\left\{\frac{X_n^l(\tau_0)}{p+\lambda_j'+\lambda_n} - \frac{\frac{6b_L}{1+b_L}}{\lambda_n(p+\lambda_j'+\lambda_n)\tilde{X}(p+\lambda_j')}\sum_{m\geqslant 1}\frac{\lambda_m X_m^l(\tau_0)}{(p+\lambda_j'+\lambda_m)}\right\} + \sum_{l=1}^{2}\sum_{j=1}^{2}\frac{P_l^2}{\prod_{\substack{i=l\\ i\neq j}}^{2}(\lambda_i'-\lambda_j')}\left\{\frac{\left(\frac{6b_L}{1+b_L}-\frac{6b_{L-1}}{1+b_{L-1}}\right)\sum_{m\geqslant 1}X_m^l(\tau_0)}{\lambda_n(p+\lambda_j'+\lambda_n)\tilde{X}(p+\lambda_j')} + \frac{8\pi\tilde{B}^l(p)}{\lambda_n(p+\lambda_j'+\lambda_n)\tilde{X}(p+\lambda_j')}\right\} \tag{25}$$

and by mathematical induction, the arbitrary nth eigenfunction of the k isotope has the form

$$\tilde{X}_n^k(p) = \sum_{l=1}^{k}\sum_{j=1}^{k}\frac{P_l^k}{\prod_{\substack{i=l\\ i\neq j}}^{k}(\lambda_i'-\lambda_j')}\left\{\frac{X_n^l(\tau_0)}{(p+\lambda_j'+\lambda_n)} - \frac{\frac{6b_L}{1+b_L}}{\lambda_n(p+\lambda_j'+\lambda_n)\tilde{X}(p+\lambda_j')}\sum_{m\geqslant 1}\frac{\lambda_m X_m^l(\tau_0)}{(p+\lambda_j'+\lambda_m)}\right\} + \sum_{l=1}^{k}\sum_{j=1}^{k}\frac{P_l^k}{\prod_{\substack{i=l\\ i\neq j}}^{k}(\lambda_i'-\lambda_j')}\left\{\frac{\left(\frac{6b_L}{1+b_L}-\frac{6b_{L-1}}{1+b_{L-1}}\right)\sum_{m\geqslant 1}X_m^l(\tau_0)}{\lambda_n(p+\lambda_j'+\lambda_n)\tilde{X}(p+\lambda_j')} + \frac{8\pi\tilde{B}^l(p)}{\lambda_n(p+\lambda_j'+\lambda_n)\tilde{X}(p+\lambda_j')}\right\}, \tag{26}$$

where $P_l^k = \prod_{j=l}^{k}\eta_{j-1}^j\lambda_{j-1}'$; $P_1^1 = 1$.

In order to isolate the second order poles in the Laplace space, Eq. (26) can be written as

$$\tilde{X}_n^k(p) = \sum_{l=1}^{k}\sum_{j=1}^{k}\frac{P_l^k}{\prod_{\substack{i=l\\ i\neq j}}^{k}(\lambda_i'-\lambda_j')}\left\{X_n^l(\tau_0)\left[\frac{1}{p+\lambda_j'+\lambda_n} - \frac{\frac{6b_L}{1+b_L}}{(p+\lambda_j'+\lambda_n)^2\tilde{X}(p+\lambda_j')}\right] - \frac{\frac{6b_L}{1+b_L}\sum_{\substack{m\geqslant 1\\ m\neq n}}\frac{\lambda_m X_m^l(\tau_0)}{(p+\lambda_j'+\lambda_m)}}{\lambda_n(p+\lambda_j'+\lambda_n)\tilde{X}(p+\lambda_j')} + \frac{\left(\frac{6b_L}{1+b_L}-\frac{6b_{L-1}}{1+b_{L-1}}\right)\sum_{m\geqslant 1}X_m^l(\tau_0)}{\lambda_n(p+\lambda_j'+\lambda_n)\tilde{X}(p+\lambda_j')} + \frac{8\pi\tilde{B}^l(p)}{\lambda_n(p+\lambda_j'+\lambda_n)\tilde{X}(p+\lambda_j')}\right\}. \tag{27}$$

Before dealing with the solution of Eq. (27), let us observe that for the case of stepwise varying conditions from Eqs. (2)–(5) it follows

$$\tilde{Q}_T^k(p) = \tilde{Q}_T'^k(p) - \tilde{N}_r^k(p) \cong \frac{4\pi}{3} a_L^3 \sum_{l=1}^{k} \frac{P_l^k}{\prod_{j=l}^{k}(p+\lambda_j')} \cdot \left[\frac{\gamma_l F}{D'} \frac{1}{p} + n_l(\tau_0) - n_r^l(\tau_0) \right], \tag{28}$$

where from Eq. (5) n_r^j is the amount of species j, released from the unit volume of the fuel in the void volume of the fuel element upto the time t_L. Also $n_j(\tau_0)$ is the amount of species j, generated inside the unit volume of the fuel up to the beginning of the time-step t_L. From Eqs. (18) and (28) the Laplace image of $B^k(\tau)$ on the time-step Δt_L is

$$\tilde{B}^k(p) = \frac{\gamma_k F'}{(1+b_L)D_L'} \frac{1}{p} - \left[\frac{a_L^3 b_L}{1+b_L} - \frac{a_{L-1}^3 b_{L-1}}{1+b_{L-1}} \right] [n_L^k - n_{r,L}^k] + \frac{a_{L-1}^3 b_{L-1}}{1+b_{L-1}} [n_{r,L}^k - n_{r,L-1}^k], \tag{29}$$

where $n_{r,L}^k(\tau_0)$ and $n_{r,L-1}^k(\tau_0)$ are the amounts of species k released from the unit volume of the fuel to the void volume of the fuel element at the beginning of the time-step t_L and at the beginning of the previous time-step t_{L-1}, respectively. If the grain volume has changed as a result of the grain growth the amounts $n_{r,L}^k$ and $n_{r,L-1}^k$ will differ accordings Eq. (4) or Eq. (4a).

Taking into account the form of Eq. (29), in order to transform Eq. (27) to the original space, we look for the originals of the following functions:

$$\begin{aligned}
\tilde{F}_n^j(p) &= \frac{1}{1+b_L} \frac{1}{(p+\lambda_j'+\lambda_n)\tilde{X}(p+\lambda_j')}, \\
\tilde{G}_n^j(p) &= \frac{1}{(p+\lambda_j'+\lambda_n)} - \frac{6b_L}{1+b_L} \frac{1}{(p+\lambda_j'+\lambda_n)^2 \tilde{X}(p+\lambda_j')}, \\
\tilde{H}_n^j(p) &= \frac{1}{1+b_L} \frac{1}{p(p+\lambda_j'+\lambda_n)\tilde{X}(p+\lambda_j')}.
\end{aligned} \tag{30}$$

Using Eqs. (29) and (30), Eq. (27) can be written as

$$\begin{aligned}
\tilde{X}_n^k(p) = \sum_{l=1}^{k} \sum_{j=1}^{k} \frac{P_l^k}{\prod_{\substack{i=l \\ i\neq j}}^{k} (\lambda_i' - \lambda_j')} \Bigg\{ & X_n^l(\tau_0) \tilde{G}_n^j(p) - \frac{6b_L}{\lambda_n} \sum_{\substack{m \geqslant 1 \\ m \neq n}} \frac{\lambda_m X_m^l(\tau_0)}{\lambda_m - \lambda_n} \left[\tilde{F}_n^j(p) - \tilde{F}_m^j(p) \right] + \frac{8\pi\gamma_l F' \tilde{H}_n^j(p)}{\lambda_n D_L} \\
& + \Bigg[\frac{b_L - b_{L-1}}{1+b_{L-1}} \sum_{m \geqslant 1} X_m^l(\tau_0) - \frac{4\pi}{3} a_{L-1}^3 b_{L-1} \Bigg[\left(\frac{a_L^3 b_L}{a_{L-1}^3 b_{L-1}} - \frac{1+b_L}{1+b_{L-1}} \right) (n_L^l - n_{r,L}^l) \\
& - \frac{1+b_L}{1+b_{L-1}} \left(n_{r,L}^l - n_{r,L-1}^l \right) \Bigg] \Bigg] \frac{6\tilde{F}_n^j(p)}{\lambda_n} \Bigg\}.
\end{aligned} \tag{31}$$

Without loosing the generality of the solution method, the well-known approximations for long times and short times can be used to calculate the originals of the functions defined by Eq. (30). Using in Eq. (20) the mathematical identity

$$\sum_{n \geqslant 1} \frac{1}{(n\pi)^2 [p + (n\pi)^2]} = \frac{1}{2p} \left[\frac{1}{3} - \left(\frac{\coth\sqrt{p}}{\sqrt{p}} - \frac{1}{p} \right) \right]$$

and taking into account that for short times, or large $p_k = p + \lambda_k'$

$$1 + 6b_L \left(\frac{1}{6} - \sum_{n \geqslant 1} \frac{p_k}{(n\pi)^2 [p + (n\pi)^2]} \right) \cong \frac{p_k + 3b_L\sqrt{p_k} - 3b_L}{p_k}$$

then we can write

$$\tilde{X}(p+\lambda_k') = \left[1 - \frac{3}{4\pi} \frac{b_L}{1+b_L} (p+\lambda_k') \sum_{n \geqslant 1} \frac{u_n^2}{(p+\lambda_k'+\lambda_n)} \right] \cong \frac{1}{1+b_L} \frac{p_k + 3b_L\sqrt{p_k} - 3b_L}{p_k}. \tag{32}$$

The zeros of Eq. (32) are

$$p_1 + \lambda_k' = z_1 = -\frac{3b_L}{2} + \sqrt{\frac{9b_L^2}{4} + 3b_L}; \quad p_2 + \lambda_k' = -z_2 = \frac{3b_L}{2} + \sqrt{\frac{9b_L^2}{4} + 3b_L}. \tag{33}$$

Now, using the notations

$$x_1 = z_1\sqrt{\tau}; \quad x_2 = z_2\sqrt{\tau}; \quad X_n = n\pi\sqrt{\tau}; \quad x_j = \sqrt{\lambda_j'\tau}; \quad \alpha_1 = \frac{x_1^3}{(x_1+x_2)(x_1^2+x_n^2)}; \quad \alpha_2 = \frac{x_2^3}{(x_1+x_2)(x_2^2+x_n^2)},$$

$$\alpha_n = \frac{x_n^2}{(x_1^2+x_n^2)(x_2^2+x_n^2)}; \quad D(x_n) = \frac{2}{\sqrt{\pi}} e^{-x_n^2} \int_0^{x_n} e^{\xi^2} d\xi,$$

$D(X_n) =$ the Dawson integral.

The originals of the functions defined by Eq. (30) are

$$F_n^j(\tau) = \begin{cases} [\alpha_n(x_n^2 + x_1x_2)\exp(-x_n^2) + \alpha_n x_n(x_1 - x_2)D(x_n) \\ +\alpha_1\ e^{x_1^2}\ \mathrm{erfc}(-x_1) + \alpha_2\ e^{x_2^2}\ \mathrm{erfc}(x_2)]\exp(-x_j^2) & \tau \leqslant 0.1, \\ 6b_L \sum\limits_{m \geqslant 1} \dfrac{\theta_m^2\ \exp[-(\theta_m^2\tau + x_j^2)]}{[\theta_m^2 - (n\pi)^2][\theta_m^2 + 9b_L(1+b_L)]} & \tau > 0.1, \end{cases}$$

$$G_n^j(\tau) = \begin{cases} \left\{1 - 6b_L\tau\left[\alpha_n(x_n^2 + x_1x_2) - \dfrac{\alpha_1}{(x_1^2+x_n^2)} - \dfrac{\alpha_2}{(x_2^2+x_n^2)}\right]\right\}\ \exp[-(x_n^2 + x_j^2)] \\ -6b_L\tau\left\{\left[\dfrac{\alpha_n(x_n^2+x_1x_2)}{2x_n} - \dfrac{\alpha_1x_1}{x_n(x_1^2+x_n^2)} + \dfrac{\alpha_2x_2}{x_n(x_2^2+x_n^2)}\right]D(x_n) + \right. \\ \left. + \dfrac{\alpha_1\ e^{x_1^2}\ \mathrm{erfc}(-x_1)}{(x_1^2+x_n^2)} + \dfrac{\alpha_2\ e^{x_2^2}\ \mathrm{erfc}(x_2)}{(x_2^2+x_n^2)} - \frac{1}{\sqrt{\pi}}\alpha_n(x_1 - x_2)\right\}\exp(-x_j^2) & \tau \leqslant 0.1, \\ \exp\left[-(x_n^2 + x_j^2)\right] + \dfrac{6b_L}{(n\pi)^2} \sum\limits_{m \geqslant 1} \dfrac{\theta_m^2\left[e^{[-(\theta_m^2\tau + x_j^2)]} - e^{[-(x_n^2+x_j^2)]}\right]}{[\theta_m^2 - (n\pi)^2]^2[\theta_m^2 + 9b_L(1+b_L)]} & \tau > 0.1, \end{cases}$$

$$H_n^j(\tau) = \begin{cases} \tau\left\{\left[-\dfrac{\alpha_n(x_n^2+x_1x_2)}{(x_n^2+x_j^2)}\exp(-x_n^2) - \dfrac{\alpha_n x_n(x_1-x_2)}{(x_n^2+x_j^2)}D(x_n) + \dfrac{\alpha_1\ e^{x_1^2}\ \mathrm{erfc}(-x_1)}{(x_1^2-x_j^2)} + \dfrac{\alpha_2\ e^{x_2^2}\ \mathrm{erfc}(x_2)}{(x_2^2-x_j^2)}\right]e^{-x_j^2} \right. \\ \left. + \left[\dfrac{\alpha_n x_n^2(x_1-x_2)}{(x_n^2+x_j^2)} - \dfrac{\alpha_1x_1}{(x_1^2-x_j^2)} + \dfrac{\alpha_2x_2}{(x_2^2-x_j^2)}\right]\dfrac{\mathrm{erf}(x_j)}{x_j} + \dfrac{\alpha_n(x_n^2+x_1x_2)}{(x_n^2+x_j^2)} - \dfrac{\alpha_1x_1}{(x_1^2-x_j^2)} - \dfrac{\alpha_2x_2}{(x_2^2-x_j^2)}\right\}, & \tau \leqslant 0.1, \\ 6b_L \sum\limits_{m \geqslant 1} \dfrac{\theta_m^2\left(1 - e^{[-(\theta_m^2\tau + x_j^2)]}\right)}{[\theta_m^2 - (n\pi)^2][\theta_m^2 + \lambda_j'][\theta_m^2 + 9b_L(1+b_L)]}, & \tau > 0.1, \end{cases}$$

where [9]

$$\theta_m = \mathrm{arctg}\left(\frac{3b_L\theta_m}{\theta_m^2 + 3b_L}\right) + m\pi; \quad m = 1, 2\ldots$$

and Eq. (31) becomes

$$X_n^k(\tau) = \sum_{l=1}^{k}\sum_{j=1}^{k} \frac{P_l^k}{\prod_{\substack{i=l \\ i\neq j}}^{k}(\lambda_i' - \lambda_j')} \left\{ X_n^l(\tau_0)G_n^j(\tau) - \frac{6b_L}{\lambda_n} \sum_{\substack{m \geqslant 1 \\ m=n}} \frac{\lambda_m X_m^l(\tau_0)}{\lambda_m - \lambda_n}[F_n^j(\tau) - F_m^j(\tau)] + \frac{8\pi\gamma_l F' H_n^j(\tau)}{\lambda_n D_L'} \right.$$
$$+ \left[\frac{b_L - b_{L-1}}{1+b_{L-1}} \sum_{m \geqslant 1} X_m^l(\tau_0) - \frac{4\pi}{3} a_{L-1}^3 b_{L-1}\left[\left(\frac{a_L^3 b_L}{a_{L-1}^3 b_{L-1}} - \frac{1+b_L}{1+b_{L-1}}\right)(n_L^l - n_{r,L}^l)\right.\right.$$
$$\left.\left. - \frac{1+b_L}{1+b_{L-1}}(n_{r,L}^l - n_{r,L-1}^l)\right]\right] \frac{6F_n^j(\tau)}{\lambda_n} \left.\right\}. \tag{34}$$

The case of only stable fission gas species ($\lambda_j' = 0,\ j = 1, 2, \ldots k$) will involve the following form of Eq. (11):

$$\frac{\partial u}{\partial \tau} = \Delta_{x_0} u + \frac{\gamma F_L'}{D_L'} - \frac{\mathrm{d}}{\mathrm{d}\tau}[bN_1(\tau)]. \tag{35}$$

Using the same mathematical formalism as described above, the eigenfunctions associated to the concentration $u(X_0, t)$ give in the Laplace space a system of algebraic coupled equations for which expressions can be obtained from Eq. (23) by simply taking $\lambda_j' = 0$ ($j = 1, 2, \ldots k$),

$$\tilde{X}_n(p) = \frac{X_n(\tau_0)}{p + \lambda_n} - \frac{\frac{6b_L}{1+b_L}}{\lambda_n(p+\lambda_n)\tilde{X}(p)} \sum_{m \geqslant 1} \frac{\lambda_m X_m(\tau_0)}{p + \lambda_m} + \frac{\left(\frac{6b_L}{1+b_L} - \frac{6b_{L-1}}{1+b_{L-1}}\right)\sum_{m \geqslant 1} X_m(\tau_0) + 8\pi\tilde{B}(p)}{\lambda_n(p+\lambda_n)\tilde{X}(p)}, \tag{36}$$

where from Eq. (29)

$$\tilde{B}(p) = \frac{\gamma \cdot F'}{(1+b_L)D'_L}\frac{1}{p} - \left[\frac{a_L^3 b_L}{1+b_L} - \frac{a_{L-1}^3 b_{L-1}}{1+b_{L-1}}\right]\cdot[n_L - n_{r,L}] + \frac{a_{L-1}^3 b_{L-1}}{1+b_{L-1}}[n_{r,L} - n_{r,L-1}]. \tag{37}$$

In a similar manner as in Eq. (30) we will define the following functions:

$$\begin{aligned}
\tilde{F}_n(p) &= \frac{1}{1+b_L}\frac{1}{(p+\lambda_n)\tilde{X}(p)},\\
\tilde{G}_n(p) &= \frac{1}{(p+\lambda_n)} - \frac{6b_L}{1+b_L}\frac{1}{(p+\lambda_n)^2\tilde{X}(p)},\\
\tilde{H}_n(p) &= \frac{1}{1+b_L}\frac{1}{p(p+\lambda_n)\tilde{X}(p)},
\end{aligned} \tag{38}$$

where

$$\tilde{X}(p) = \left[1 - \frac{3}{4\pi}\frac{b_L}{1+b_L}p\sum_{n\geqslant 1}\frac{u_n^2}{(p+\lambda_n)}\right].$$

Substituting Eqs. (38) and (37) in Eq. (36) after the separation of the second order poles, Eq. (36) becomes

$$\begin{aligned}
\tilde{X}_n(p) &= X_n(\tau_0)\tilde{G}_n(p) - \frac{6b_L}{\lambda_n}\sum_{\substack{m\geqslant 1\\ m\neq n}}\frac{\lambda_m X_m(\tau_0)}{\lambda_m - \lambda_n}[\tilde{F}_n(p) - \tilde{F}_m(p)] + \frac{8\pi\gamma F'\tilde{H}_n(p)}{\lambda_n D'_L}\\
&\quad + \left[\frac{b_L - b_{L-1}}{1+b_{L-1}}\sum_{m\geqslant 1}X_m(\tau_0) - \frac{4\pi}{3}a_{L-1}^3 b_{L-1}\left[\left(\frac{a_L^3 b_L}{a_{L-1}^3 b_{L-1}} - \frac{1+b_L}{1+b_{L-1}}\right)(n_L - n_L^r) - \frac{1+b_L}{1+b_{L-1}}(n_L^r - n_{L-1}^r)\right]\right]\frac{6\tilde{F}_n(p)}{\lambda_n}.
\end{aligned} \tag{39}$$

The originals of Eq. (38) are,

$$F_n(\tau) = \begin{cases} \alpha_n(x_n^2 + x_1x_2)\ \mathrm{e}^{-x_n^2} + \alpha_n x_n(x_1 - x_2)D(x_n) + \alpha_1\ \mathrm{e}^{x_1^2}\mathrm{erfc}(-x_1) + \alpha_2\ \mathrm{e}^{x_2^2}\ \mathrm{erfc}(x_2), & \tau \leqslant 0.1,\\ 6b_L\sum_{m\geqslant 1}\dfrac{\theta_m^2\exp[-\theta_m^2\tau]}{[\theta_m^2 - (n\pi)^2][\theta_m^2 + 9b_L(1+b_L)]}, & \tau > 0.1, \end{cases}$$

$$G_n(\tau) = \begin{cases} \left\{1 - 6b_L\tau\left[\alpha_n(x_n^2 + x_1x_2) - \dfrac{\alpha_1}{(x_1^2 + x_n^2)} - \dfrac{\alpha_2}{(x_2^2 + x_n^2)}\right]\right\}\mathrm{e}^{-x_n^2} - 6b_L\tau\left\{\left[\dfrac{\alpha_n(x_1 - x_2)(2x_n^2 + 1)}{2x_n}\right.\right.\\ \quad \left.\left. - \dfrac{\alpha_1 x_1}{x_n(x_1^2 + x_n^2)} + \dfrac{\alpha_2 x_2}{x_n(x_2^2 + x_n^2)}\right]D(x_n) + \dfrac{\alpha_1\ \mathrm{e}^{x_1^2}\ \mathrm{erfc}(-x_1)}{(x_1^2 + x_n^2)} + \dfrac{\alpha_2\ \mathrm{e}^{x_2^2}\ \mathrm{erfc}(x_2)}{(x_2^2 + x_n^2)} - \dfrac{\alpha_n(x_1 - x_2)}{\sqrt{\pi}}\right\}, & \tau \leqslant 0.1,\\ \exp(-x_n^2) + \dfrac{6b_L}{(n\pi)^2}\sum_{m\geqslant 1}\dfrac{\theta_m^2[\mathrm{e}^{-\theta_m^2\tau} - \mathrm{e}^{-x_n^2}]}{[\theta_m^2 - (n\pi)^2]^2[\theta_m^2 + 9b_L(1+b_L)]}, & \tau > 0.1, \end{cases}$$

$$H_n(\tau) = \begin{cases} \tau\left[-\dfrac{\alpha_n(x_n^2 + x_1x_2)\ \mathrm{e}^{-x_n^2}}{x_n^2} - \dfrac{\alpha_n(x_1 - x_2)D(x_n)}{x_n} + \dfrac{\alpha_1\ \mathrm{e}^{x_1^2}\ \mathrm{erfc}(-x_1)}{x_1^2} + \dfrac{\alpha_2\ \mathrm{e}^{x_2^2}\ \mathrm{erfc}(x_2)}{x_2^2}\right], & \tau \leqslant 0.1,\\ 6b_L\sum_{m\geqslant 1}\dfrac{\theta_m^2(1 - \mathrm{e}^{-\theta_m^2 tau})}{[\theta_m^2 - (n\pi)^2][\theta_m^2 + 9b_L(1+b_L)]}, & \tau > 0.1. \end{cases}$$

Thus the original function of Eq. (39) is

$$\begin{aligned}
X_n(\tau) &= X_n(\tau_0)G_n(\tau) - \frac{6b_L}{\lambda_n}\sum_{\substack{m\geqslant 1\\ m\neq n}}\frac{\lambda_m X_m(\tau_0)}{\lambda_m - \lambda_n}[F_n(\tau) - F_m(\tau)] + \frac{8\pi\gamma F' H_n(\tau)}{\lambda_n D'_L}\\
&\quad + \left[\frac{b_L - b_{L-1}}{1+b_{L-1}}\sum_{m\geqslant 1}X_m(\tau_0) - \frac{4\pi}{3}a_{L-1}^3 b_{L-1}\left[\left(\frac{a_L^3 b_L}{a_{L-1}^3 b_{L-1}} - \frac{1+b_L}{1+b_{L-1}}\right)(n_L - n_L^r) - \frac{1+b_L}{1+b_{L\text{-}1}}(n_L^r - n_{L-1}^r)\right]\right]\frac{6F_n(\tau)}{\lambda_n}.
\end{aligned} \tag{40}$$

From Eqs. (13), (14) and (16) the total amount of species k which remain inside the average volume grain after the volatile fission products diffusion simultaneously with grain growth and grain boundary resolution is

$$N^k(t_L) = \frac{1}{1+b_L}\sum_{m\geqslant 1}X_m^k(t_L) + \frac{b_L}{1+b_L}[Q_T^k(t_L) - N_r^k(t_L)]. \tag{41}$$

The knowledge of the number of the volatile fission products $N^k(t_L)$, from the average volume grain, along with Eqs. (1) and (4) or Eq. (4a), allows one to evaluate at any time the amount of volatile fission product of species k, either arrived at the grain boundary or released in the void volume of the fuel element.

As a result of the local thermal gradients, the fuel microcracking along the grain boundaries could arise during the fast fuel cooling in those regions where large grain boundary areas are covered with fission gas bubbles. Specialised thermomechanical codes could give information about these regions from the fuel pellets.

Also the rising of a continuous network of interconnected tunnels where the gas is vented all the time out of the grain boundary could be associated to a sequence of incubation times no smaller than the smallest time-step chosen for calculation.

In both cases described, the diffusion equation associated to the fission products migration is the same as Eq. (6) but, because the function changes given by Eqs. (9) and (9′), it is necessary to change the initial condition to

$$X_n^k(0) = X_n^k(t_{L-1}) + u_n^2 \frac{3b_{L-1}}{4\pi} N_l^k(t_{L-1}) \tag{42}$$

as a result of the boundary condition changes to the perfect sink one (the correction parameter becomes $b_L = 0$).

3. Application and discussion of the results and of other similar models

To illustrate the results of the evaluation method described above on the volatile fission products behaviour during the fuel irradiation, we use the same model of calculating the surface density of the saturation number of atoms of the stable fission gases from the grain boundary as described in Refs. [9,10,12]. At stationary equilibrium with the external forces on the grain boundary, the surface concentration of the gas atoms arrived inside the intergranular bubbles at boundary saturation n^{sat}, can be calculated supposing the bubbles to be identical, lenticular shaped pores comprising spherical caps of fixed coalescence radius in the plane of the grain boundary with diedhral angles $2\theta = 100°$ [9,10],

$$n^{\text{sat}} = \frac{4 f_c f(\theta) r_b}{3 k_B T \sin^2\theta} \left[\frac{2\gamma}{r_b} + P_{\text{ext}} \right], \tag{43}$$

where $f(\theta) = 1 - (3/2)\cos\theta + (1/2)\cos^3\theta$, and f_c is the coverage fraction at grain boundary saturation (we taken it as 1 in the following discussion), γ the surface tension of the bubble (0.6 J/m^2), k_B the Boltzmann constant (J/K), T the fuel temperature (K), r_b the bubble radius (0.5 μm), P_{ext} is the hydrostatic pressure (Pa).

To reduce the number of the parameters involved in fission product behaviour inside the fuel oxide, the hydrostatic pressure has been assumed to be zero in the present analyses.

The expression of the diffusion coefficient has been taken from Ref. [17]. The neutronic parameters used (decay constant, fission yields, etc.)have been taken from Ref. [15].

Using Eqs. (1)–(4), (40)–(42) along with the assumption that the kinetics of migration of the stable fission gas species governs the intergranular gas bubble nucleation, growth and interlinkage, the amount of any volatile species that migrated at the boundary of the fuel grains or in the void volume of the fuel element can be calculated with a high accuracy for any kind of irradiation history. Dividing the power history in small time-steps of constant irradiation conditions (constant grain size, constant temperature, etc.) the solutions can be extended for both slower and fast power transients (Figs. 11–14). The kinetics of volatile fission products migration depend on the diffusion parameters, the irradiation induced resolution and chemical properties of the nuclide of interest and on its precursors [4]. That is, the results presented in the following are only qualitative and only an effective diffusion coefficient along with the irradiation induced resolution corresponding to stable gas species are considered.

Further comparisons with the experimental results to give the adequate weights of the model parameter are necessary. The accuracy of the method described depends on the number of the eigenfunctions $X_n(t)$, given by Eq. (34) for radioactive products and Eq. (40) for stable gas species. Comparisons with the analytical solutions described in Ref. [12] of the stable gas species behaviour using a constant correction parameter of the same range of the values as used for all the temperature histories from the present analysis shown that one hundred functions are enough for a calculation relative error smaller than 10^{-4}.

An important result of all the analyses presented here is the strong dependence of the kinetics of gas diffusion on the correction parameter. The theoretical treatment of irradiation induced resolution in the model presented by Speight, introduces the resolution layer depth λ, and the resolution parameter b' as physical parameters of resolution. If the resolution parameter can be defined using Eq. (8), we have no information about the λ parameter other than Ref. [10] where its values are taken to be between 10^{-8} and 10^{-5} m. In the following discussion we have fixed $\lambda = 10^{-8}$ m.

The correction parameter is a function of the fuel temperature and it varies by about three order of magnitude. Thus, because of its dependence on the diffusion coefficient, the correction parameter will change exponentially with the fuel temperature and this feature becomes important during fuel transients. During the constant temperature histories (Figs. 1–10), it depends linearly on the grain size changes Eq. (8′) and will increase to about two times at 1400°C and three times at 1600°C up to the end of the irradiation history (500 MWh/kgU at 60 kW/m linear power). As already pointed out [15], when the grain growth is considered, the equilibrium between the fission products diffused at the grain

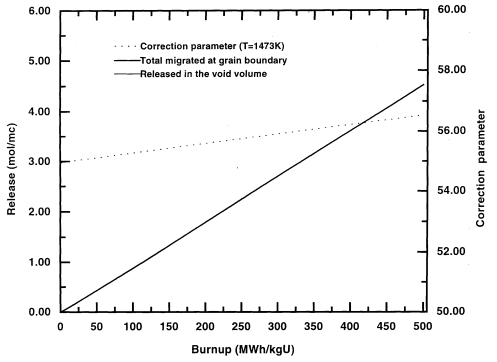

Fig. 1. Evolution of the concentration of the stable gas species in the void volume of the fuel element and total cumulated value in both void volume and at the grain boundary along with the correction parameter changes, during a constant temperature history (1200°C).

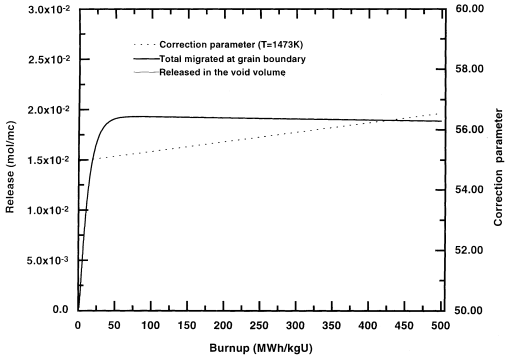

Fig. 2. Evolution of the concentration of the ^{133}Xe species in the void volume of the fuel element and total cumulated value in both void volume and at the grain boundary along with the correction parameter changes, during a constant temperature history (1200°C).

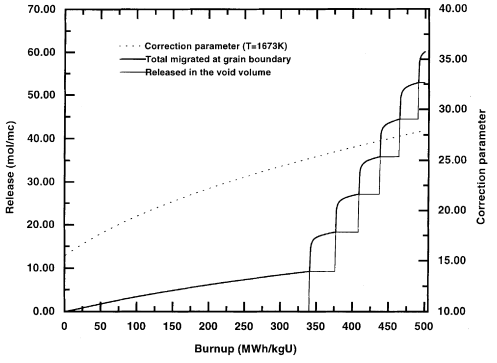

Fig. 3. Evolution of the concentration of the stable gas species in the void volume of the fuel element and total cumulated value in both void volume and at the grain boundary along with the correction parameter changes, during a constant temperature history (1400°C).

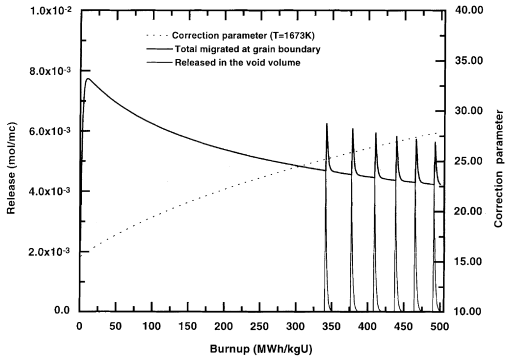

Fig. 4. Evolution of the concentration of the ^{133}I species in the void volume of the fuel element and total cumulated value in both void volume and at the grain boundary along with the correction parameter changes, during a constant temperature history (1400°C).

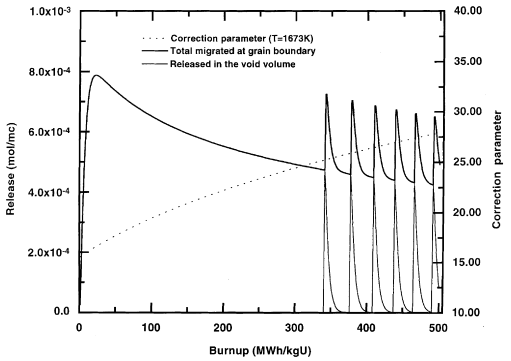

Fig. 5. Evolution of the concentration of the ^{133m}Xe species in the void volume of the fuel element and total cumulated value in both void volume and at the grain boundary along with the correction parameter changes, during a constant temperature history (1400°C).

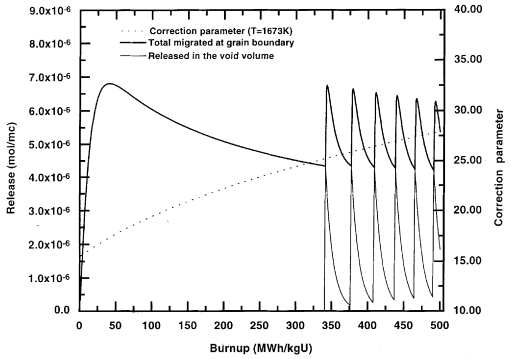

Fig. 6. Evolution of the concentration of the ^{133}Xe species in the void volume of the fuel element and total cumulated value in both void volume and at the grain boundary along with the correction parameter changes, during a constant temperature history (1400°C). The precursors contribution has been neglected.

boundary and the total generated inside the fuel grains cannot be reached. This can be seen in Figs. 2, 4–8 and 10 where the time evolution for some constant temperature irradiation histories are depicted. Only at 1200°C (Fig. 2) a quasi-stationary state of ^{133}Xe evolution can be observed. Because the correction parameter depends linearly on the grain size which is almost constant, it does not change significantly at a fuel temperature of 1200°C and this can be followed in Fig. 2. Moreover, there is no fission gas release in the void volume of the fuel element during the whole irradiation

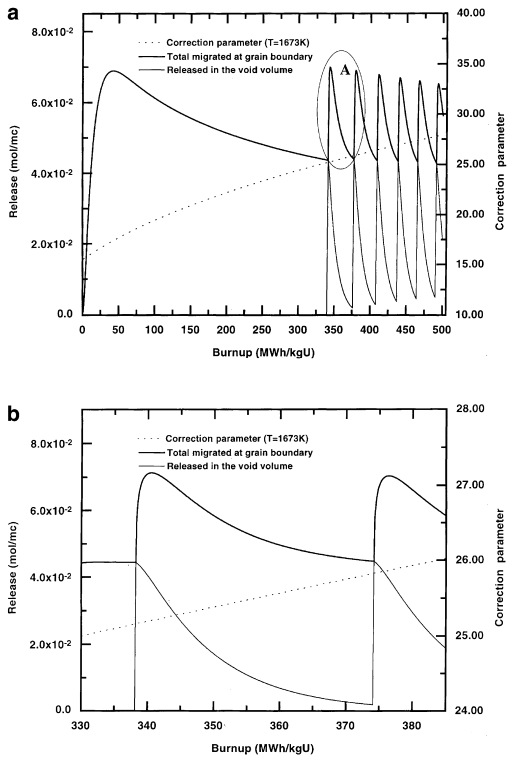

Fig. 7. (a) Evolution of the concentration of the ^{133}Xe species in the void volume of the fuel element and total cumulated value in both void volume and at the grain boundary along with the correction parameter changes, during a constant temperature history (1400°C). (b). Detail A corresponding to Fig. 7(a) for ^{133}Xe.

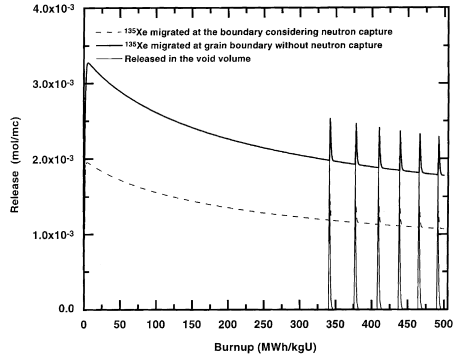

Fig. 8. Evolution of the concentration of the ^{135}Xe species in the void volume of the fuel element and total cumulated value in both void volume and at the grain boundary along with the correction parameter changes, during a constant temperature history (1400°C).

history at 1200°C. At 1400°C the first intergranular bubble coalescence (the first incubation time) is reached at 340 MWh/kgU and it slowly goes down at ~70 MWh/kgU for 1600°C temperature history.

The kinetics of the fission products behaviour become more complex versus the cases presented in Ref. [15] where only the irradiation induced resolution has been neglected. Because the boundary condition Eq. (7) becomes zero after every intergranular bubble coalescence, a fast release of the gas atoms from the grain surface to the grain boundary can be observed and the grain boundary saturation with gas atoms is reached shortly after the bubble interlinkage (Figs. 3 and 9). Figs. 4–8 show the behaviour of the volatile fission products ^{133}I, ^{133m}Xe, ^{133}Xe, without the contribution of its precursors, the total ^{133}Xe, and respectively ^{135}Xe with and without its decaying by neutron absorption during the constant 1600°C temperature history. Versus the time evolution depicted in Fig. 3 corresponding to the stable fission

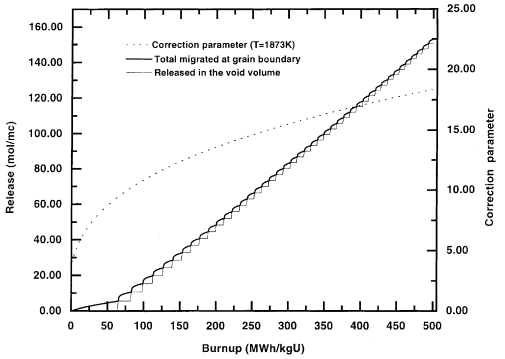

Fig. 9. Evolution of the concentration of the stable gas species in the void volume of the fuel element and total cumulated value in both void volume and at the grain boundary along with the correction parameter changes, during a constant temperature history (1600°C).

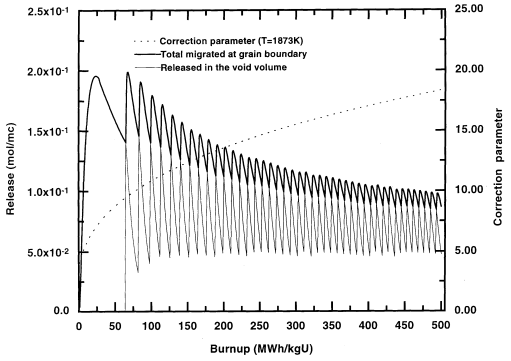

Fig. 10. Evolution of the concentration of the ^{133}Xe species in the void volume of the fuel element and total cumulated value in both void volume and at the grain boundary along with the correction parameter changes, during a constant temperature history (1600°C).

products and function of the decay properties of the above mentioned isotopes, peaks of various forms arise, representing their amount any time after the intergranular bubble coalescence. An interesting situation can be observed in Fig. 10, where as a result of reducing of the incubation times, even if the saturation state at the grain boundary is not reached, the lowest amount of ^{133}Xe released in the void volume of the fuel element is almost constant during the irradiation history.

Figs. 11–14 show the kinetics of release of both stable gas species and ^{133}Xe, during a slower transient (7 days at 60 kW/m after 100 MWh/kgU at 1000°C) and a fast ramp (30′ at 60 kW/m after 300 MWh/kgU at 1000°C), respectively. For both these temperature histories, the saturation condition is reached and ~36 mol/m^3 fission gas are released at the end of the slower transient (Fig. 11) at ~1850° C and respectively ~14 mol/m^3 at the end of the fast ramp (Fig. 13) at ~1950°C in the void volume of the fuel element. Also, along with the stable gas species about 0.7 mol/m^3 ^{133}Xe during the slower transient history (Fig. 12) and 0.1 mol/m^3 ^{133}Xe during the fast ramp history (Fig. 14) are released. A high amount of fission gas (~150 mol/m^3) is released shortly after the fuel temperature increasing from 1400°C to 1600°C and this can be seen in Fig. 15(a) and b and analogously for ^{133}Xe in Fig. 16(a) and (b). The behaviour of the volatile fission products during transients can be explained following the change of the correction parameter as a result of the temperature increases. Thus, at 1400°C the assumption that the successive saturation with gas atoms at the grain boundary for time-steps smaller than the time-step chosen for calculation (~1 MWh/KgU) implies the rising of a network of intergrannular tunnels at the grain boundary which is equivalent to the nullifying of the correction parameter b as can be seen in Fig. 15(a) and Fig. 16(a) versus Fig. 15(b) and Fig. 16(b) respectively. As it can be seen the kinetics of the fission gas release are however quite different.

An apparently unexpected situation can be followed in Fig. 17(a) where a decreasing temperature history is depicted. Because the fuel temperature decreases from 1800°C to 1600°C the irradiation induced resolution will dominate the fission gas diffusion at the grain boundary. A higher amount of gas atoms will be turned back to the fuel matrix rather

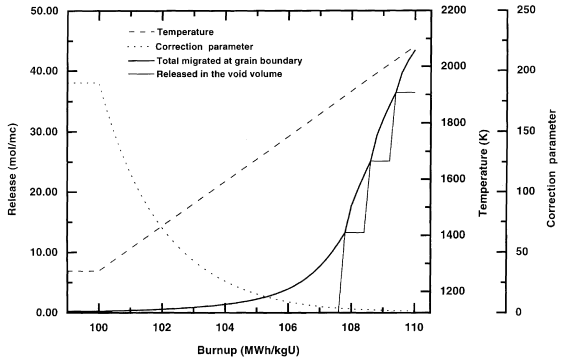

Fig. 11. Evolution of the concentration of the stable gas species in the void volume of the fuel element and total cumulated value in both void volume and at the grain boundary along with the correction parameter changes, during a slower temperature transient (7 days at 60 kW/m).

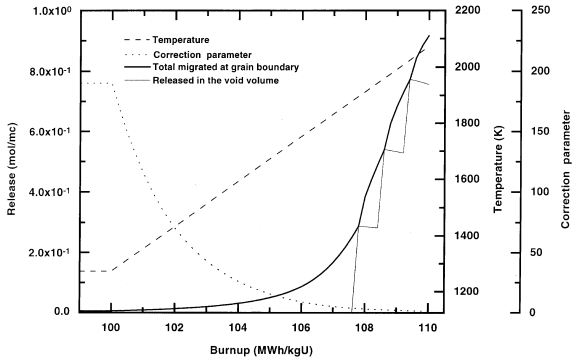

Fig. 12. Evolution of the concentration of the ^{133}Xe species in the void volume of the fuel element and total cumulated value in both void volume and at the grain boundary along with the correction parameter changes, during a slower temperature transient (7 days at 60 kW/m).

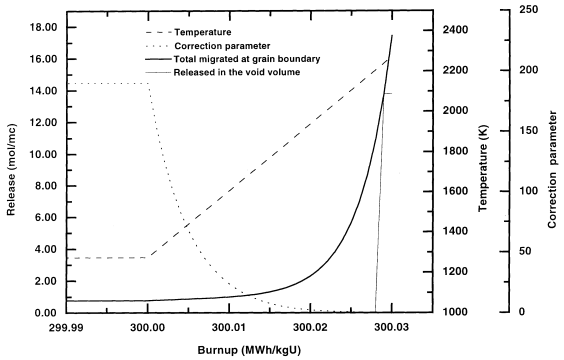

Fig. 13. Evolution of the concentration of the stable gas species in the void volume of the fuel element and total cumulated value in both void volume and at the grain boundary along with the correction parameter changes, during a short temperature transient (30 min at 60 kW/m).

than being diffused at the same time at the grain boundary. A detail of this behaviour is shown in Fig. 17(b) and similar situations for ^{133}Xe can be seen in Fig. 18(a) and (b). After the equilibrium is settled, the fission gas slowly increases on the grain boundary and the saturation condition is reached again only after ~70 MWh/kgU. Because the fuel tem-

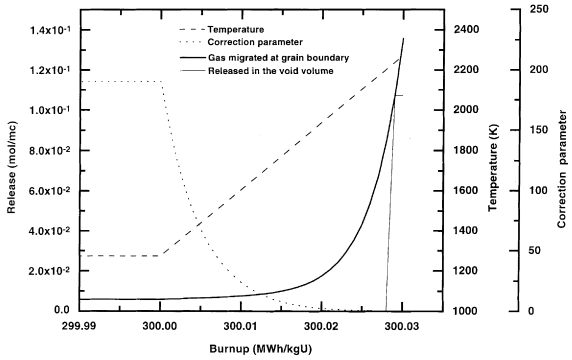

Fig. 14. Evolution of the concentration of the ^{133}Xe species in the void volume of the fuel element and total cumulated value in both void volume and at the grain boundary along with the correction parameter changes, during a short temperature transient (30 min at 60 kW/m).

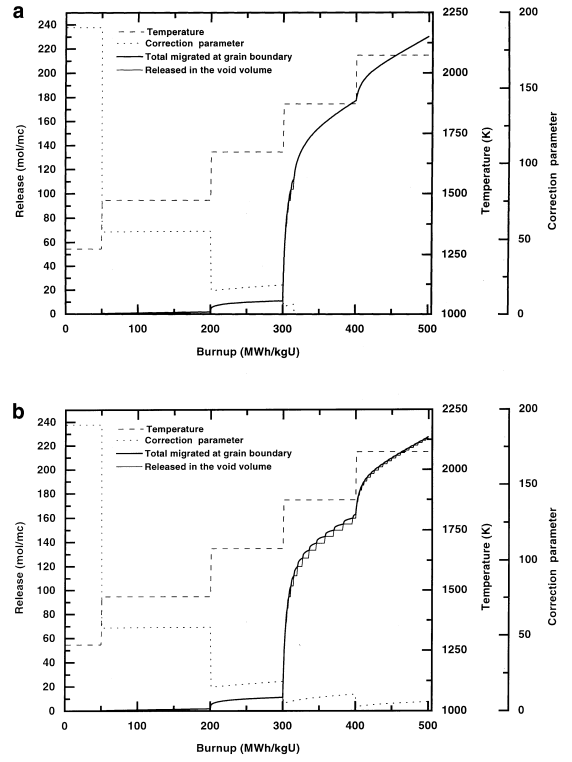

Fig. 15. (a). Evolution of the concentration of the stable gas species in the void volume of the fuel element and total cumulated value in both void volume and at the grain boundary along with the correction parameter changes, during an increasing temperature history (considering that a permanent network of interconnecting tunnels has been formed). (b). Evolution of the concentration of the stable gas species in the void volume of the fuel element and total cumulated value in both void volume and at the grain boundary along with the correction parameter changes, during an increasing temperature history.

perature decreases up to the end of irradiation, the correction parameter of gas resolution will strongly increase from $b = 1.4$ at the beginning of irradiation (1800°C fuel temperature), to $b = 1073$ at the end of irradiation (1000°C fuel temperature). It has been shown in Ref. [12] that as a result of the large domains of values of the resolution layer depth λ and of the resolution parameter b' it is difficult to associate a constant value of the correction parameter for gas resolution when an arbitrary irradiation history is studied. The method described above becomes useful because the only unknown parameter for gas resolution at the grain boundary is the resolution layer depth of the volatile fission

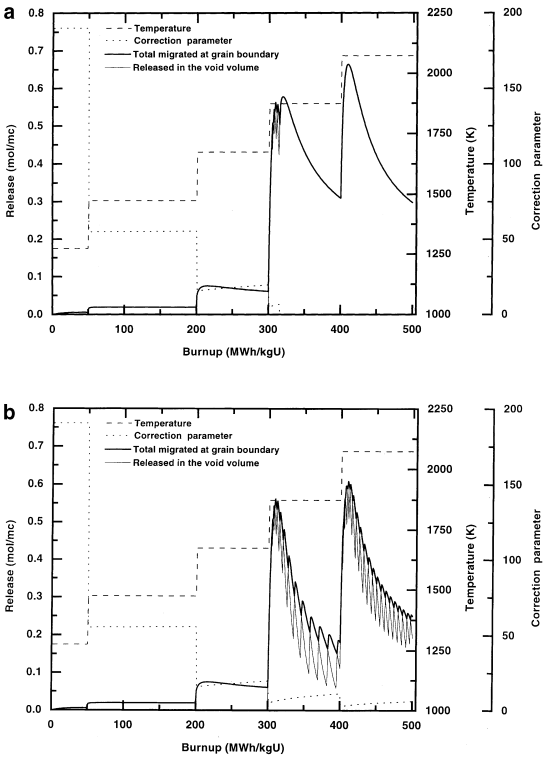

Fig. 16. (a). Evolution of the concentration of the ^{133}Xe species in the void volume of the fuel element and total cumulated value in both void volume and at the grain boundary along with the correction parameter changes, during an increasing temperature history (considering that a permanent network of interconnecting tunnels has been formed). (b). Evolution of the concentration of the ^{133}Xe species in the void volume of the fuel element and total cumulated value in both void volume and at the grain boundary along with the correction parameter changes, during an increasing temperature history.

products. Moreover, the results presented above suggest that the values $\lambda > 10^{-8}$ m will give in effect lower amounts of fission gas release. Obviously, only by calibration with the experimental results, the method could become a powerful device to evaluate the volatile fission products behaviour during fuel irradiation. Other processes such as fuel stoichiometry changes, fuel microcracking, can be easily quantified for every temperature-controlled or grain growth-controlled time-step and their weights can be calculated by adequate changes of the diffusion coefficient or the boundary condition for gas diffusion. The thermodynamically induced resolution at the grain boundary of the volatile fission products is also an important parameter and it can be easily considered by adding a concentration-dependent term to Eq. (6) in the same manner as that used by Turnbull and Friskney [4].

In attempting to improve the Notley and Hastings model [25], McDonald et all. [22], solve the diffusion equation

$$\frac{\partial C^k}{\partial t} = \nabla(D_k \nabla C^k) - \lambda_k C^k + \gamma_k F + \eta^k_{k-1}\lambda_{k-1} C^{k-1}, \tag{44}$$

$$C^k[a(t), t] = 0, \tag{44a}$$

that was derived from the mass balance of the diffusing species k, applied to arbitrary fixed systems.

They added artificially a term to Eq. (44), proportional to $((3\ \mathrm{d}a)/(a\mathrm{d}t))$ (the sweeping contribution [22]) and transformed Eq. (44) to a fixed volume by using the variable changes in spherical symmetry $x \sim r/a(t)$. El-Saied and Olander extended the solution of Eq. (44) to a grain volume distribution function [13] and Forsberg, et al., gave a solution of Eq. (44) considering the irradiation induced resolution of the stable fission gas species at the grain boundary as time dependent [18], applying the rule chain of differentiation [13] to the function $C^k(r,t) \to C^k(x(t), t)$ as previously introduced by McDonald et al. [22].

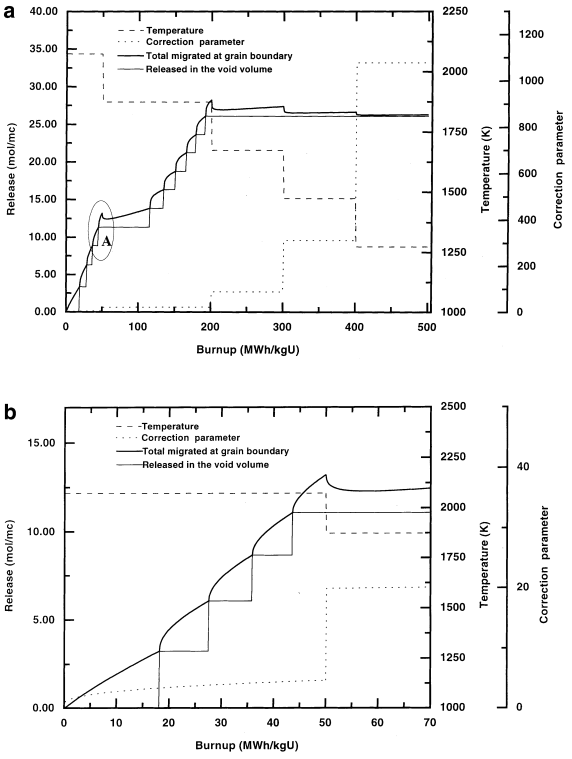

Fig. 17. (a) Evolution of the concentration of the stable gas species in the void volume of the fuel element and total cumulated value in both void volume and at the grain boundary along with the correction parameter changes, during a decreasing temperature history. (b). Detail A corresponding to Fig. 17(a), for stable gas species.

But Eq. (44) does not describe adequately the diffusion from the fuel grains simultaneously with the grain growth. It results from the mass balance of a diffusing species in any fixed region inside the fuel grains but not simultaneously on the entire grain volume that change in time as a result of the grain growth.

The adequate theoretical description of this problem has been given in Refs. [11,12,15] and also some supplementary criticisms have been done in Ref. [21]. As for example [21], to use the spatial coordinate as independent of time in a time dependent domain, as it results from the condition (44a), it is necessary to give a supplementary definition of the concentration beyond the grain boundary, to maintain its continuity by both at the left and at right hand of the boundary, any time, as it is the case of the Newman's problem [23,24].

To illustrate the discrepancies between the two manners of work, the above described solution method of Eq. (6) along with the initial and boundary conditions (7) and (9′) has been used to evaluate the fission gas release (FGR) from a region of the fuel where the material parameters, the irradiation conditions and the temperature history are identical with those described in Ref. [18]. For comparison, in Fig. 19(a) and (b) are shown the results published in Ref. [18]. The difference between the Fig. 19(a) and b is only the time-step chosen for FGR evaluation, using the mathematical formalism presented above. Thus in Fig. 19(a) a time-step of 5 h was used, while in Fig. 19(b) the time-step was of 1 h.

The differences of the FGR predictions between the two models are very small for the case of constant size grain during the irradiation, but they increase when simultaneous grain growth is considered. Thus for the case of the step function of the temperature history chosen in Ref. [18] whose parameters are 2000 h at 1000°C and then a ramp at 1600°C for 200 h, the amount of FGR predicted using the above described model is with about 2 mol/m^3 greater than the FGR from Ref. [18] and almost equal for the case of constant size grain. The stability of solutions (40) and (41) it is obvious from the results depicted in Fig. 19(a) and (b), where for the two different time-steps the results are not significantly changed.

The continuous line of FGR in Fig. 19(a) and b shown the FGR evolution after a succession of time-steps of the grain boundary saturation, for which the correction parameter becomes zero. Consequently, the boundary condition for gas diffusion is nullified as it was discussed above (Fig. 15(a) and (b)) but the differences in FGR predictions are insignificantly.

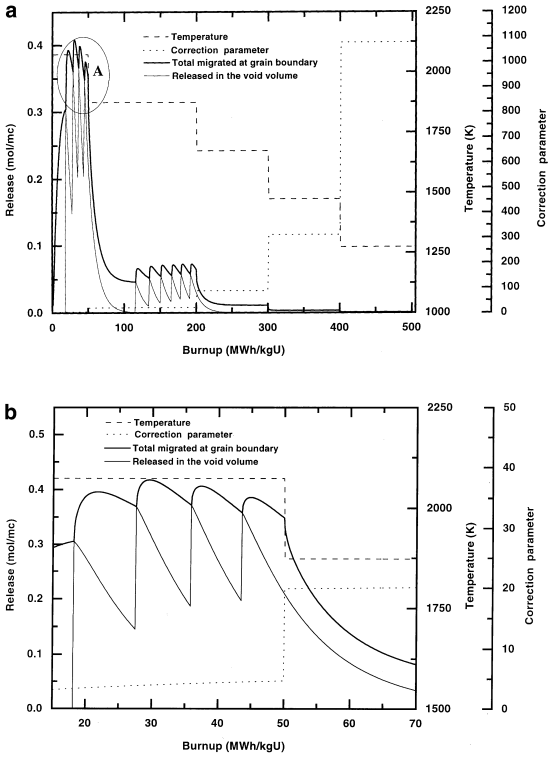

Fig. 18. (a) Evolution of the concentration of the ^{133}Xe species in the void volume of the fuel element and total cumulated value in both void volume and at the grain boundary along with the correction parameter changes, during a decreasing temperature history. (b). Detail A corresponding to the evolution of the ^{133}Xe species from Fig. 18(a).

4. Conclusions

It has been shown that treating the average volume grain of the fuel oxide as a thermodynamically homogeneous closed subsystem, the mathematical formulation of the diffusion problem associated with the volatile fission products migration at the grain boundary permits analytical solutions considering their direct yield from fission or from precursors simultaneously with the grain growth and the grain boundary resolution during both the steady state and transient fuel irradiation conditions. In order to simplify the solution method a correction parameter for fission gas resolution at the grain boundary has been defined. It depends on both irradiation induced resolution and the surface to volume ratio of the fuel grains that can be evaluated from the average volume grain or using the real grain volume distribution function of the fuel oxide.

The significant changes of the correction parameter during all irradiation histories analysed involve fast changes of the volatile fission products amount at the grain boundary especially during temperature transients. Because the correction parameter depends on the grain size, the diffusion coefficient and the fission rate, it will change on a large scale and cannot be considered constant when the real irradiation histories are simulated. The times of the intergranular bubble interlinkage and the FGR from the grain boundary into the void volume are also important parameters in the volatile fission products evolution on the grain boundary. Short time after the intergranular bubble interlinkage the boundary conditions for fission gas diffusion will change to a perfect sink one and the fission products will easily migrate from the grain surface resolution layer to the grain boundary. This mechanism accelerates the intergranular bubble nucleation and growing. During the decreasing temperature histories the gas resolution becomes faster than the gas diffusion at the grain boundary and the fission gas is absorbed rather in the grain surface than remaining inside the intergranular bubbles.

Comparison with the other published models show their inadequate statement of the problem when the volatile fission products diffusion from the fuel grains simultaneously with the grain growth in polycrystals in analysed.

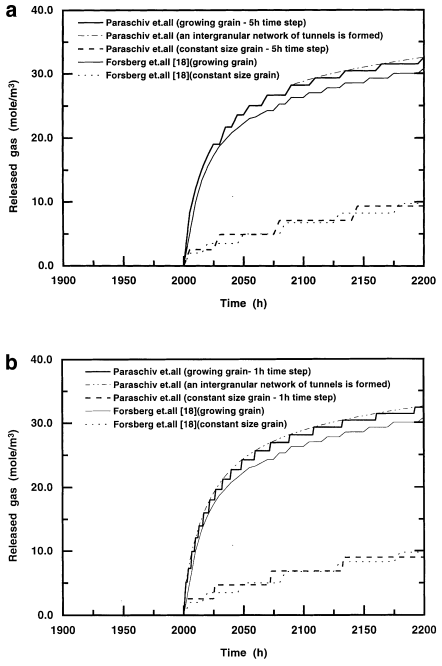

Fig. 19. (a). Fission gas release as a function of time after a discontinuous raise in fuel temperature(ramp) to (1600°C). Comparison between two models. (b). Fission gas release as a function of time after a discontinuous raise in fuel temperature(ramp) to (1600°C). Comparison between two models.

Acknowledgements

This paper has been carried out in part under an International Atomic Energy Agency Research Contract.

We would like to thank to Dr Pierre Chantoin from the IAEA Division of Nuclear Fuel Cycle and Waste Management for constant help of the project development and the IAEA Department of Research and Isotopes for prompt administrative assistance of the research.

The authors would like to thank also, for useful discussions during the paper development, Professor Dr G. Ciobanu from the University of Bucharest, Faculty of Physics.

Appendix A

From Eq. (19) and using expression (21), we have to solve a system of n coupled equations of the form

$$X_1 + a_1 \sum_{j=1}^{n} X_j = R_j; \quad a_1 = -\frac{3}{4\pi} \frac{b_L}{1+b_L} \frac{u_1^2 (p+\lambda_k')}{(p+\lambda_k'+\lambda_1)} \tag{A.1}$$

or

$$\begin{aligned}
&(1+a_1)X_1 + a_1X_2 + a_1X_3 + \ldots + a_1X_n = R_1,\\
&a_2X_1 + (1+a_2)X_2 + a_2X_3 + \ldots + a_2X_n = R_2,\\
&a_3X_1 + a_3X_2 + (1+a_3)X_3 + \ldots + a_3X_n = R_3,\\
&a_nX_1 + a_nX_2 + a_nX_3 + \ldots + (1+a_n)X_n = R_n,
\end{aligned} \tag{A.2}$$

of which determinant is

$$\Delta = \begin{vmatrix} 1+a_1 & a_1 & a_1 & \dots & a_1 \\ a_2 & 1+a_2 & a_2 & \dots & a_2 \\ a_3 & a_3 & 1+a_3 & \dots & a_3 \\ : & : & : & : & : \\ a_n & a_n & a_n & : & 1+a_n \end{vmatrix} = \begin{vmatrix} 1+\sum_{k=1}^{n} a_k & 1+\sum_{k=1}^{n} a_k & 1+\sum_{k=1}^{n} a_k & \dots & 1+\sum_{k=1}^{n} a_k \\ a_2 & 1+a_2 & a_2 & \dots & a_2 \\ a_3 & a_3 & 1+a_3 & \dots & a_3 \\ : & : & : & : & : \\ a_n & a_n & a_n & \dots & 1+a_n \end{vmatrix}$$

$$= \left(1+\sum_{k=1}^{n} a_k\right) \cdot \begin{vmatrix} 1 & 1 & 1 & \dots & 1 \\ a_2 & 1+a_2 & a_2 & \dots & a_2 \\ a_3 & a_3 & 1+a_3 & \dots & a_3 \\ : & : & : & : & : \\ a_n & a_n & a_n & : & 1+a_n \end{vmatrix} = \left(1+\sum_{k=1}^{n} a_k\right) \cdot \begin{vmatrix} 1 & 0 & 0 & \dots & 0 \\ a_2 & 1 & 0 & \dots & 0 \\ a_3 & 0 & 1 & \dots & 0 \\ : & : & : & : & : \\ a_n & 0 & 0 & : & 1 \end{vmatrix} = \left(1+\sum_{k=1}^{n} a_k\right).$$

Using the Cramer method,

$$X_k = \frac{\Delta_{X_k}}{\Delta}, \tag{A.3}$$

it follows

$$\Delta_{X_k} = \begin{vmatrix} 1+a_1 & a_1 & \dots & R_1 & \dots & a_1 \\ a_2 & 1+a_2 & \dots & R_2 & \dots & a_2 \\ : & : & : & : & : & : \\ a_k & a_k & \dots & R_k & \dots & a_k \\ : & : & : & : & : & : \\ a_n & a_n & \dots & R_n & \dots & 1+a_n \end{vmatrix} = \begin{vmatrix} 1+a_1 & -1 & \dots & R_1 & \dots & -1 \\ a_2 & 1 & \dots & R_2 & \dots & 0 \\ : & : & : & : & : & : \\ a_k & 0 & \dots & R_k & \dots & 0 \\ : & : & : & : & : & : \\ a_n & 0 & \dots & R_n & \dots & 1 \end{vmatrix}$$

$$= (-1)^{k+k} R_k \begin{vmatrix} 1+a_1 & -1 & \dots & -1 & \dots & -1 \\ a_2 & 1 & \dots & 0 & \dots & 0 \\ : & : & : & : & : & : \\ a_{k+1} & 0 & \dots & 1 & \dots & 0 \\ : & : & : & : & : & : \\ a_n & 0 & \dots & 0 & \dots & 1 \end{vmatrix} + (-1)^{1+k} a_k \begin{vmatrix} -1 & -1 & \dots & R_1 & \dots & -1 \\ 1 & 0 & \dots & R_2 & \dots & 0 \\ : & : & : & : & : & : \\ 0 & 0 & \dots & R_{k+1} & \dots & 0 \\ : & : & : & : & : & : \\ 0 & 0 & \dots & R_n & \dots & 1 \end{vmatrix} =$$

$$= (-1)^{2k} R_k \begin{vmatrix} 1+\sum_{\substack{i=1 \\ i\neq k}}^{n} a_i & 0 & \dots & 0 & \dots & 0 \\ a_2 & 1 & \dots & 0 & \dots & 0 \\ : & : & : & : & : & : \\ a_{k+1} & 0 & \dots & 1 & \dots & 0 \\ : & : & : & : & : & : \\ a_n & 0 & \dots & 0 & \dots & 1 \end{vmatrix} + (-1)^{1+k} a_k \begin{vmatrix} 0 & 0 & \dots & \sum_{\substack{i=1 \\ i\neq k}}^{n} R_i & \dots & 0 \\ 1 & 0 & \dots & R_2 & \dots & 0 \\ : & : & : & : & : & : \\ 0 & 0 & \dots & R_{k+1} & \dots & 0 \\ : & : & : & : & : & : \\ 0 & 0 & \dots & R_n & \dots & 1 \end{vmatrix}$$

$$= (-1)^{2k} R_k \left(1+\sum_{\substack{i=1 \\ i\neq k}}^{n} a_i\right) + (-1)^{1+k} a_k (-1)^k \sum_{\substack{i=1 \\ i\neq k}}^{n} R_i$$

and from (A.3),

$$X_k = R_k - a_k \frac{\sum_{i=1}^{n} R_i}{\left(1+\sum_{i=1}^{n} a_i\right)}. \tag{A.4}$$

Because both the index k and n are arbitrary chosen the system (A.2) can be extended to an infinity equations and Eq. (A.4) is the same for any $k = 1, 2, \dots$

References

[1] D.R. Olander, Fundamental Aspects of Nuclear Reactor Fuel Elements, ERDA, USA, 1976, p. 314.
[2] M.V. Speight, Nucl. Sci. Eng. 37 (1969) 180.
[3] J.A. Turnbull, J. Nucl. Mater. 50 (1974) 63.
[4] J.A. Turnbull, C.A. Friskney, J. Nucl. Mater. 58 (1975) 31.
[5] C.A. Friskney, M.V. Speight, J. Nucl. Mater. 62 (1976) 89.
[6] J.A. Turnbull, C.A. Friskney, F.A. Johnson, A.J. Walter, J.R. Findlay, J. Nucl. Mater. 67 (1977) 301.
[7] C.A. Friskney, J.A. Turnbull, F.A. Johnson, A.J. Walter, J.R. Findlay, J. Nucl. Mater. 68 (1977) 186.
[8] M.V. Speight, J.A. Turnbull, J. Nucl. Mater. 68 (1977) 244.
[9] K. Forsberg, A.R. Massih, J. Nucl. Mater. 135 (1985) 140.
[10] D.M. Dowling, R.J. White, M.O. Tucker, J. Nucl. Mater. 110 (1982) 37.
[11] M. Paraschiv, A. Paraschiv, J. Nucl. Mater. 185 (1991) 182.
[12] M. Paraschiv, A. Paraschiv, J. Nucl. Mater. 195 (1992) 138.
[13] U.M. El-Saied, D.R. Olander, J. Nucl. Mater. 207 (1993) 313.
[14] M.C. Paraschiv, A. Paraschiv, F. Glodeanu, J. Nucl. Mater. 246 (1997) 223.
[15] M.C. Paraschiv, A. Paraschiv, J. Nucl. Mater. 218 (1994) 66.
[16] A.D. Wapham, Philos. Mag. 23 (1971) 987.
[17] P.A. Jackson, J.A. Turnbull, R.J. White, IAEA-TCM on Water Reactor Fuel Element Computer Modelling in Steady-State, Transient and Accident Conditions, Preston, England, 19–22 September, 1988.
[18] K. Forsberg, F. Lindstrom, A.R. Massih, IAEA TECDOC-957, August 1997.
[19] A.H. Booth, CRTC-721 (957).
[20] R. Hargreaves, D.A. Collins, J. Br. Nucl. Energy Soc. 15 (Oct. 4) (1976) 311–318.
[21] M.C. Paraschiv, AECL - Memorandum to I.J. Hastings, R.D. Mc Donald, J.R. Walker, 1992 February 27, Final Report IAEA 6198/1992.
[22] L.D. McDonald, D.B. Duncan, B.J. Lewis, F.C. Iglesias, AECL 9810 (1989).
[23] H.S. Carlsaw, J.C. Jaeger, Conduction of Heat in Solids; Oxford University, Oxford, 1948.
[24] J. Crank, The Mathematics of Diffusion, Oxford University, Oxford, 1955.
[25] M.J.F. Notley, I.J. Hastings, Nucl. Eng. Design 56 (1980) 163.